Journal of Glaciology (2017), **63**(241) 929–935 doi: 10.1017/jog.2017.59

^{239,240}Pu and ^{236}U records of an ice core from the eastern Tien Shan (Central Asia)

CHAOMIN WANG,[1] SHUGUI HOU,[1,2] HONGXI PANG,[1] YAPING LIU,[3] HEINZ WALTER GÄGGELER,[4,5] MARCUS CHRISTL,[6] HANS-ARNO SYNAL[6]

[1]*School of Geographic and Oceanographic Sciences, Nanjing University, 210023 Nanjing, China*
[2]*CAS Center for Excellence in Tibetan Plateau Earth Sciences, Beijing 100101, China*
[3]*State Key Laboratory of Cryospheric Sciences, Northwest Institute of Eco-Environment and Resources, Chinese Academy of Sciences, 730000 Lanzhou, China*
[4]*Paul Scherrer Institut, 5232 Villigen PSI, Switzerland*
[5]*Department of Chemistry and Biochemistry, University of Bern, 3000 Bern, Switzerland*
[6]*Laboratory of Ion Beam Physics, ETH Zürich, 8093 Zürich, Switzerland*
Correspondence: Heinz Walter Gäggeler <heinz.gaeggeler@psi.ch>; Shugui Hou <shugui@nju.edu.cn>

ABSTRACT. Radioisotopes (^{239}Pu, ^{240}Pu, ^{236}U) formed during atmospheric nuclear weapons testing (NWT) can be used for dating and therefore be applied as markers of the beginning of the Anthropocene Epoch. Moreover, ^{240}Pu/^{239}Pu ratios enable source identification (general fallout, local emission sources). Ice core segments from a 57.6 m ice core to bedrock from eastern Tien Shan, China were selected for ^{239,240}Pu and ^{236}U analyses by using compact low-energy accelerator mass spectrometry. The observed ^{240}Pu/^{239}Pu atom ratios were 0.18 ± 0.02, with one exception, indicating global fallout. No evidence for emissions from the nearby local sources Lop Nor was observed. The total deposition rates during NWT for ^{239}Pu and ^{240}Pu amount to 1.55 × 10^{9} atoms·cm^{-2} and 3.1 × 10^{8} atoms·cm^{-2}, respectively. With the higher undisturbed fallout of ^{239}Pu compared with values reported for glaciers from European Alps at Col du Dome and Colle Gnifetti as well as from the polar region, the eastern Tien Shan glacier would be an ideal site for defining the start of the Anthropocene. ^{236}U is a rather new environmental tracer, while little is known about its global fallout from NWT. The observed deposition flux of ^{236}U during NWT amounts to 3.5 × 10^{8} atoms·cm^{-2} at the drill site. The average ^{236}U/^{239}Pu ratio of 0.27 ± 0.09 is in good agreement with literature values from global fallout.

KEYWORDS: glacier chemistry, ice core, mountain glaciers

1. INTRODUCTION

Recently there have been debates about the definition and the start of the Anthropocene regarding human alterations of Earth's environments (Zalasiewicz and others, 2014; Lewis and Maslin, 2015; Monastersky, 2015). The long-lived ^{239}Pu nuclide was suggested to be considered as a globally synchronous stratigraphic marker for defining the beginning of the Anthropocene (Waters and others, 2015). In 2009, at the 35th International Geological Congress in South Africa, the Anthropocene Working Group (AWG) first advised the International Commission on Stratigraphy (ICS) on the possibility of formally adding the Anthropocene as an interval to the International Chronostratigraphic Chart. Anthropocene was first suggested to reflect pervasive human alternations of Earth's environments (Crutzen and Stoermer, 2000; Crutzen, 2002). Since then, there have been increasing debates about defining the Anthropocene and finding the stratigraphic markers that reflect the human impacts on Earth (Waters and others, 2014, 2016; Lewis and Maslin, 2015; Monastersky, 2015; Ruddiman and others, 2015; Zalasiewicz and others, 2015). Recent indications are that the Great Acceleration marked by a dramatic increase in human population, large changes in natural processes (Steffen and others, 2007; Canfield and others, 2010; Wolfe and others, 2013) and an enhanced production of new human-made materials such as plastics, organic and inorganic pollutants (Ford and others, 2014) since the 1950s has the highest support within the AWG for defining the beginning of the Anthropocene (Waters and others, 2015; Zalasiewicz and others, 2015). The long-lived ^{239}Pu nuclide resulting from the fallout of nuclear weapons testing (NWT) was subsequently suggested as the marker for a globally synchronous stratigraphic boundary for the mid-20th century (Monastersky, 2015; Waters and others, 2015; Zalasiewicz and others, 2015).

Plutonium in the air is now dominated by atmospheric discharge from nuclear weapons tests and the re-suspension of plutonium-bearing soil particles (Choppin and Morgenstern, 2001). Extensive nuclear weapon tests were conducted by the USA and the former Soviet Union in the mid-20th century, and tests on a smaller scale were done later by the UK, France, China and India, leading to the most fallout of plutonium in the atmosphere during 1945–1962. The global fallout of plutonium concentration peak in sediments marked as 1963 in the northern atmosphere has commonly been used to construct the time sequence of lacustrine sediments (Ketterer and others, 2004) and ice cores (Olivier and others, 2004; Wendel and others, 2013). Besides dating, plutonium isotope ratios, especially ^{240}Pu/^{239}Pu ratios have been used to differentiate the plutonium contribution from general fallout from other emission sources.

Depending on emission source, the ^{240}Pu/^{239}Pu atom ratios vary significantly. It is well known (Krey and others, 1976; Perkins and Thomas, 1980; Koide and others, 1985) that this ratio has a value of about 0.18 if the plutonium fallout stems from the NWT by US and Soviet tests that ejected the debris far into the stratosphere followed by transfer to the Earth surface within 1–2 years by sedimentation and wet precipitation. ^{240}Pu/^{239}Pu ratios from nuclear weapon-grade materials range from 0.01 to 0.07 (Micholas and others, 1992). Values from nuclear reactors are up to 0.4 or even higher (Chamizo and others, 2008).

In addition, recent interest mostly from marine scientists arose in ^{236}U as a tracer for modelling ocean circulation (Sakaguchi and others, 2012; Winkler and others, 2012). The reason is the extremely conservative behaviour of this radionuclide in the marine environment that makes it an ideal tracer for such studies. The average residence time of uranium in a marine environment in the form of $UO_2(CO_3)_3^{4-}$ is expected to be very long, about 0.3–0.5 million years (Bloch, 1980; Dunk and others, 2002). One drawback for application of this 'new' tracer in environmental research is, however, the poor knowledge of its deposition rates on the Earth surface. ^{236}U was mostly ejected into the atmosphere during NWT. Estimated values are ~1 tonne (Sakaguchi and others, 2009). Other sources of anthropogenic ^{236}U are the reprocessing plants in La Hague and Sellafield, respectively, with a total release of ~100 kg (Casacuberta and others, 2014; Christl and others, 2015a). The amount of natural ^{236}U is much lower, ~35 kg (Steier and others, 2008). This results in an estimated pre-anthropogenic ^{236}U/^{238}U value of $\approx 10^{-13}$ in ocean water (Christl and others, 2012).

In 2005, two ice cores to drilled bedrock (58.7 m for core 1 and 57.6 m for core 2) were recovered from a dome on the Miaoergou Glacier, eastern Tien Shan, Central Asia (43°03′19″N, 94°19′21″E, 4512 m a.s.l.) (Fig. 1). In Liu and others (2011), a dating was suggested down to 17 m for core 2 based on annual layer counting of the assumed seasonality of δ^{18}O and crustal species (Ca^{2+}, Ba^{2+}). Moreover, a total β activity measurement was performed that depicted two peaks at ~10.5 and 12.5 m depth, respectively. The maximum at 12.5 m depth was assigned to the nuclear weapons fallout peak in 1963 and the younger maximum at 10.5 m to possible fallout from the nearby Chinese nuclear test site Lop Nor, which is at a distance of ~400 km SW of the glacier drill site. From 16 October 1964 to 29 July 1996, 23 atmospheric and 22 underground nuclear tests were conducted at Lop Nor (Yang and others, 2000). Later, an additional dating was performed using ^{210}Pb (Wang and others, 2014). This measurement enabled to date the core down to 41.5 m. In general, the agreement between the two dating attempts was observed, though the accuracy was rather limited with a time resolution of no more than ~5 years.

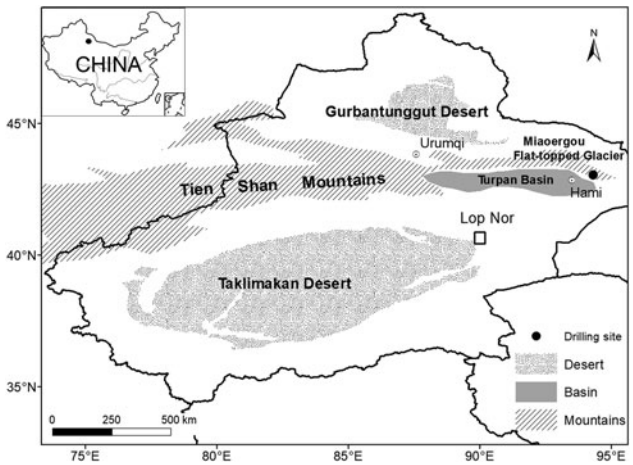

Fig. 1. Location of the Miaoergou flat-topped glacier in eastern Tien Shan, China. The black dot shows the position of the drilling site (43°03′19″N, 94°19′21″E, 4512 m a.s.l.).

Later discussions questioned the assignment of the first β activity peak found in Liu and others (2011) to fallout from Lop Nor. In order to verify this assignment, we decided to analyse the ^{240}Pu/^{239}Pu atomic ratio for the segment of the core that exhibited increased total β activity, hence between ~8 and 15 m depth. The ^{236}U analysis was also included in order to increase knowledge on ^{236}U deposition rates. So far, only one ^{236}U measurement exists using an ice core from Svalbard (Wendel and others, 2013). It is well known that fallout from NWT exhibits a significant deposition rate dependence as a function of latitude. Hence, the measured value from (Wendel and others, 2013) at 79.83°N of 1.63×10^8 atoms·cm^{-2} does not represent expected values at mid- or low latitudes, which underlies the request for additional measurements in non-polar areas.

Given the extremely low concentrations of all three radionuclides (^{239,240}Pu and ^{236}U) in ice from glaciers, the highest sensitivity is required for their analysis. This prerequisite is met best by accelerator mass spectrometry (AMS). Only one out of the three radionuclides, ^{239}Pu, has so far been measured in ice cores with another mass spectrometric technique, ICP-SFMS (Gabrieli and others, 2011; Arienzo and others, 2016).

2. EXPERIMENTAL

2.1. Ice core treatment

The ice cores were transported in a frozen state after drilling to the State Key Laboratory of Cryospheric Sciences, Chinese Academy of Sciences in Lanzhou. For further analysis, the 57.6 m long ice core – also analysed for ^{210}Pb (Wang and others, 2014) – was used. The core segments from 8 to 15 m depth were cut into 11 0.5–1 m long pieces. Each piece weighted between ~1 and 2 kg. The core segments were then subjected to chemical treatment, first in Lanzhou (part a) and then at Bern University (part b), prior to measurement of the wanted radionuclides at the AMS facility at ETH Zürich, see below.

2.2. Chemical treatment

Part (a)

Each ice sample was melted and acidified to pH <1 with HNO_3 (65%) of ultrapure quality. The solutions were stored for ~12 h (overnight) and then filtered to remove mineral dust. A 100 mg $KMnO_4$ (dissolved in H_2O) was added and left for 30 min in order to oxidize all Pu species to the oxidation state VI. Subsequently, $NaOH_{conc}$ was added until pH reached a value of ~9. Then, 200 mg $NaHSO_3$ (dissolved in H_2O) was added to form MnO_2 and left for ~1 h to let the precipitate settle. The precipitate was filtered through a membrane filter. The solution was subjected again to the entire procedure as described above and both precipitates were stored in a plastic container for

transport to Switzerland. The chemical treatment closely followed a described procedure from (Olivier, 2004).

Part (b)

Both filters of each sample were dissolved in 20 mL 1 M HNO_3 together with 100 mg Mohr's salt [$(NH_4)_2Fe(SO_4)_2{\cdot}6H_2O$]. Twenty microlitres of ^{233}U and 100 µL ^{242}Pu tracers were added to the solution. The standards contained 91.29 pg·g^{-1} ^{233}U and 9.16 pg·g^{-1} ^{242}Pu, respectively. Hence, the total amounts of added standards were 1.826 pg ^{233}U and 0.916 pg ^{242}Pu, respectively. It was therefore assumed that the chemical treatment described in part (a) was quantitative (100% yield).

Then 20 mL concentrated HNO_3 and 0.5 g $NaNO_2$ were added and the solution gently heated until the formation of nitrous gases stopped.

Purification and preparation of Pu for AMS measurement

A DIONEX 1 × 8 column (6 g) was pre-conditioned with 40 mL 8 M HNO_3. The solution from above was loaded onto the column, then the beaker rinsed four times with 10 mL 8 M HNO_3 and all solutions eluted through the column. All eluates were combined for further preparation of uranium (see below).

The column was then rinsed with 50 mL HCl_{conc} to remove traces of Fe, Am, Th and Ca prior to eluting Pu with 50 mL freshly prepared 0.1 M NH_4I/9 M HCl solution. The eluate was evaporated to dryness, fumed three times with 5 mL HNO_3/0.5 mL HCl_{conc} and then three times with 5 mL HCl_{conc}. The residue was taken up with 2 mL HCl_{conc} and then 7 mL H_2O added that contained 1 mg Fe^{3+}. Twenty-five per cent NH_3 solution was added dropwise until $Fe(OH)_3$ precipitation formed. Through heating in a water bath, the pH was reduced to a value between 8 and 9. The precipitate was centrifuged for 15 min and the supernatant decanted. The precipitate was dried in an oven at 100 °C for 2 h, and then transferred to 1.5 mL Eppendorf vials.

This part of the chemical separation also closely followed a procedure described by Olivier (2004).

Purification and preparation of U for AMS measurement

A UTEVA column (0.5 g; 100–150 m) was preconditioned with 3 M HNO_3. The *U* solution in 8 M HNO_3 from above was loaded onto the column. *U* was eluted from the column with 30 mL 0.01 M HCl and the eluate evaporated to dryness. The residue was taken up with 2 mL HCl_{conc} followed by the same procedure as described above for Pu.

2.3. AMS measurement

The AMS measurements of ^{236}U and Pu isotopes were performed with the compact low-energy system Tandy at ETH Zürich. The system is well suited for the sensitive detection of ultra-trace amounts of actinides. Details of the AMS setup for actinide measurements have been described previously (Christl and others, 2013). The compact AMS system at ETH Zürich combines high transport efficiency (35–40% transmission) (Vockenhuber and others, 2011) with the highest abundance sensitivity (of the order of 10^{-12}) (Christl and others, 2015b), so that detection limits at the sub-femtogram level can be reached for the actinides (Dai and others, 2011) even if an intense potential interference is present on a neighbouring mass (e.g. ^{238}U interfering with ^{239}Pu or ^{235}U with ^{236}U).

Measured ^{236}U/^{233}U (Pu-isotopic) ratios were normalized to the ETH Zürich in house standard ZUTRI (CNA) (Christl and others, 2013) and corrected for impurities carried by the ^{233}U (^{242}Pu) tracer. The reported one sigma uncertainties (Table 1) take into account counting statistics, the scatter of the isotopic ratios during repeated measurements of the same sample, the uncertainty of standard normalization and the uncertainty of the blank correction.

Pu isotopes were measured in both, the Pu and U fraction of the ice core samples (Table 1). While the ^{240}Pu/^{239}Pu ratios were indistinguishable in both fractions (Table 3), the ^{x}Pu/^{242}Pu ratios (x = 239, 240) in those fractions were significantly different for some samples. Possible explanations for this observation are described below.

The fact that during chemical preparation the Pu spike obviously did not behave like the Pu isotopes in the sample makes the straight forward application of the isotope dilution method for the calculation of Pu concentrations impossible. Nevertheless, concentrations of Pu isotopes in each fraction could be estimated using the following procedure. To make different AMS runs (U and Pu fractions) comparable, the counting rate of the in house CNA standards was used for

Table 1. Concentrations of ^{239}Pu, ^{240}Pu and ^{236}U in the Miaoergou ice core (uncertainties represent counting statistics (1 σ))

Sample	Depth	Mass	^{239}Pu[a]	^{240}Pu[a]	^{239}Pu[b]	^{240}Pu[b]	^{236}U
	m	G	fg·kg^{-1}	fg·kg^{-1}	fg·kg^{-1}	fg·kg^{-1}	fg·kg^{-1}
1	8–9	2055	113 ± 4	22 ± 1	205 ± 6	41 ± 2	106 ± 3
2	9–9.5	1230	448 ± 9	82 ± 2	n.d.[c]	n.d.[c]	105 ± 6
3	9.5–10	1272	2018 ± 44	392 ± 9	n.d.[c]	n.d.[c]	624 ± 30
4	10–10.5	1255	2410 ± 65	432 ± 21	–[d]	–[d]	–[d]
5	10.5–11	1264	1137 ± 19	228 ± 7	25 ± 1	5 ± 0.2	434 ± 12
6	11–11.5	1018	703 ± 16	145 ± 3	228 ± 6	45 ± 1	174 ± 10
7	11.5–12	1148	677 ± 10	134 ± 4	410 ± 9	79 ± 2	465 ± 19
8	12–12.5	1324	722 ± 20	142 ± 4	1628 ± 31	314 ± 6	616 ± 17
9	12.5–13	1242	598 ± 9	113 ± 2	996 ± 19	186 ± 4	345 ± 11
10	13–14	2439	173 ± 4	46 ± 2	562 ± 13	147 ± 3	89 ± 3
11	14–15	2205	90 ± 2	14 ± 0.4	1.4 ± 0.1	0.24 ± 0.03	20 ± 2

[a] Concentration of plutonium in the plutonium fraction.
[b] Concentration of plutonium in the uranium fraction.
[c] No Pu was detected in the uranium-fraction.
[d] Sample lost due to technical problems during chemical separation.

Table 2. Total ^{239}Pu, ^{240}Pu and ^{236}U concentrations and activities

Sample	Depth	^{239}Pu	^{239}Pu	^{240}Pu	^{240}Pu	^{236}U	^{236}U
	m	fg·kg^{-1}	mBq·kg^{-1}	fg·kg^{-1}	mBq·kg^{-1}	fg·kg^{-1}	mBq·kg^{-1}
1	8–9	318 ± 7	0.7 ± 0.02	63 ± 2	0.5 ± 0.02	106 ± 3	0.25 ± 0.007
2	9–9.5	448 ± 9	1.0 ± 0.02	82 ± 2	0.7 ± 0.02	105 ± 6	0.25 ± 0.014
3	9.5–10	2018 ± 44	4.6 ± 0.1	392 ± 9	3.3 ± 0.08	624 ± 30	1.49 ± 0.072
4	10–10.5	2410 ± 65	5.5 ± 0.15	432 ± 21	3.6 ± 0.18	–[a]	–[a]
5	10.5–11	1163 ± 19	2.7 ± 0.04	233 ± 7	2.0 ± 0.06	434 ± 12	1.04 ± 0.029
6	11–11.5	931 ± 17	2.1 ± 0.04	190 ± 3	1.6 ± 0.03	174 ± 10	0.42 ± 0.024
7	11.5–12	1087 ± 14	2.5 ± 0.03	213 ± 4	1.8 ± 0.03	465 ± 19	1.11 ± 0.045
8	12–12.5	2350 ± 37	5.4 ± 0.08	456 ± 7	3.8 ± 0.06	616 ± 17	1.47 ± 0.041
9	12.5–13	1594 ± 21	3.7 ± 0.05	298 ± 4	2.5 ± 0.03	345 ± 11	0.82 ± 0.026
10	13–14	735 ± 13	1.7 ± 0.03	193 ± 3	1.6 ± 0.03	89 ± 3	0.21 ± 0.007
11	14–15	92 ± 2	0.2 ± 0.005	14 ± 0.4	0.1 ± 0.003	20 ± 2	0.05 ± 0.005

[a] Sample lost due to technical problems during chemical separation.

normalization. Under the assumption that no ^{242}Pu was lost during chemical preparation (all ^{242}Pu is found either in the U or Pu fraction), the amount of ^{242}Pu present in either fraction was estimated for each sample by comparing the normalized average counting rates of ^{242}Pu during each (U and Pu) run. With the estimated amounts of ^{242}Pu in each respective fraction, the isotopic dilution method now could be applied to calculate ^{239}Pu and ^{240}Pu concentrations in the U and Pu fractions separately (Table 1). The uncertainty of this estimation is most probably larger than the reported analytical uncertainties reported in Tables 1–3. However, it cannot be easily estimated since it rather represents a systematic error affecting the accuracy of the results. To get an impression of the uncertainty associated with the above described procedure, it was applied twice for some samples. The results of the two independent experiments differ by 15% on average.

3. RESULTS AND DISCUSSIONS

The measurements were performed for: (i) the samples prepared as described above, (ii) for spike samples and (iii) for blank samples in a well-defined protocol. This enabled measurement at the highest possible level of accuracy and under clean conditions.

Therefore, Table 1 which first lists the total weight of each sample then summarizes all results of the 11 ice core segments. This not only includes measured concentrations of ^{239}Pu, ^{240}Pu and ^{236}U in the corresponding chemical fractions, but also ^{239}Pu and ^{240}Pu concentrations in the ^{236}U fraction. The reason why after absolutely identical chemical procedures part of plutonium was found in the uranium fraction is unclear. A tentative assumption is that in some samples, part of plutonium did exist in an unexpected chemical form.

Table 2 lists the total mass values for ^{239,240}Pu and for ^{236}U in each segment, but also gives the resulting activities. The reason is that in the literature, published data have been presented sometimes in mass units and sometimes in activity values. Therefore, comparing our results with literature values becomes easier.

The total ^{239}Pu concentration along the ice core is depicted in Figure 2. It clearly shows a double peak structure. We assign the maximum at ~10.5 m to fallout from ~1963, while the maximum at ~12.5 m is assigned to the pre-moratorium fallout peaking at ~1958. In the previous work by Liu and others (2011), the total β activity peak assigned at ~12.5 m to fallout from 1963 should be modified and the annual layer counting result in that work was overestimated by ~5 years. In Figures 2 and 3, we applied the new time scale as best guess from the annual layer counting, the ^{210}Pb dating (Wang and others, 2014) and the nuclear weapons fallout (Pu&U) peaks at 1963 and 1958 in the same ice core, respectively. The uncertainty for each date is estimated

Table 3. ^{240}Pu/^{239}Pu (at·at^{-1}), ^{236}U/^{239}Pu (at·at^{-1}) and ^{239}Pu/^{242}Pu (at·at^{-1}) ratios

Sample	Depth	^{240}Pu/^{239}Pu[a]	^{240}Pu/^{239}Pu[b]	^{236}U/^{239}Pu[b]	^{239}Pu/^{242}Pu[a]	^{239}Pu/^{242}Pu[b]
	m	at·at^{-1}	at·at^{-1}	at·at^{-1}	at·at^{-1}	at·at^{-1}
1	8–9	0.19 ± 0.01	0.20 ± 0.01	0.34 ± 0.01	0.34 ± 0.01	1.96 ± 0.06
2	9–9.5	0.18 ± 0.01	–[c]	–[c]	0.61 ± 0.01	–[c]
3	9.5–10	0.19 ± 0.01	–[c]	–[c]	2.84 ± 0.06	–[c]
4	10–10.5	0.18 ± 0.01	–[d]	–[d]	3.34 ± 0.09	–[d]
5	10.5–11	0.20 ± 0.01	0.20 ± 0.01	0.38 ± 0.01	1.63 ± 0.03	1.29 ± 0.04
6	11–11.5	0.21 ± 0.01	0.20 ± 0.01	0.19 ± 0.01	1.06 ± 0.02	1.02 ± 0.03
7	11.5–12	0.20 ± 0.01	0.19 ± 0.01	0.43 ± 0.02	1.00 ± 0.02	3.67 ± 0.08
8	12–12.5	0.20 ± 0.01	0.19 ± 0.01	0.27 ± 0.01	1.39 ± 0.04	9.95 ± 0.19
9	12.5–13	0.19 ± 0.01	0.19 ± 0.01	0.22 ± 0.01	1.06 ± 0.02	6.04 ± 0.11
10	13–14	0.27 ± 0.01	0.26 ± 0.01	0.12 ± 0.01	0.69 ± 0.02	4.65 ± 0.11
11	14–15	0.15 ± 0.01	0.17 ± 0.02	0.23 ± 0.02	0.23 ± 0.004	0.09 ± 0.01

[a] ^{240}Pu/^{239}Pu or ^{239}Pu/^{242}Pu in the plutonium fraction.
[b] ^{240}Pu/^{239}Pu, ^{236}U/^{239}Pu or ^{239}Pu/^{242}Pu in the uranium fraction.
[c] Pu was not detectable in U fraction.
[d] Uranium fraction was lost.

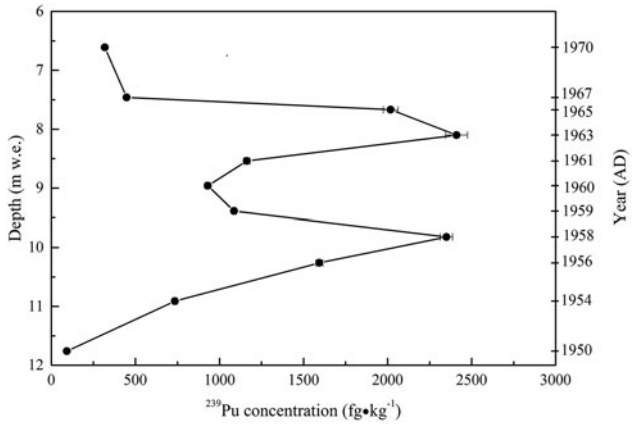

Fig. 2. Concentrations of ^{239}Pu in the Miaoergou ice core as a function of depth (left axis). The right axis indicates the 'best guess' age (see text). Error bars refer to 1 σ.

as ±1 year. From the two time markers, an approximate annual average deposition rate of 25.4 cm results, or ~20.5 cm w.e., in good agreement with the values of 22.9 cm w.e. observed for a much longer time period, 1851–2005 AD (Wang and others, 2014).

The total deposition of ^{239}Pu integrated over the NWT period amounts to 1.55×10^9 atoms·cm^{-2}, obtained from the data summarized in Table 1 and the diameter of the ice core of 9.4 cm. This value is higher compared with values reported for glaciers from the European Alps with 0.9×10^9 atoms·cm^{-2} at Col du Dome, a site close to Mont Blanc in France and 0.7×10^9 atoms·cm^{-2} at Colle Gnifetti, Swiss Alps (Gabrieli and others, 2011) but lower than 3.6×10^9 atoms·cm^{-2} obtained from an analysis of an ice core at Belukha, Altai (Russia) (Olivier and others, 2004). Other literature values are 1.7×10^9 measured in a Greenland ice core (Koide and others, 1982) or 0.54×10^9 at the Agassiz ice cap (Kudo and others, 2000), respectively. In a recent publication (Arienzo and others, 2016), a comparison was made between ^{239}Pu concentration in Arctic and Antarctic samples, indicating that they differ by about a factor of three (Northern hemisphere (NH) to Southern hemisphere ratio). The maximum value for ^{239}Pu from several Arctic sites (~5 mBq·kg^{-1}) agrees well with our maximum value of 5.5 mBq·kg^{-1} (see Table 2).

All values listed above for the total flux of ^{239}Pu during NWT in NH vary within a factor of about seven and do not scale with latitude. This indicates that local influences such as annual deposition rates, altitude, wind erosion, dry/wet deposition significantly influence the inventories. With the higher fallout of ^{239}Pu in the mid-latitudes, the ice cores from the eastern Tien Shan and Altai may be very suitable for defining the beginning of Anthropocene.

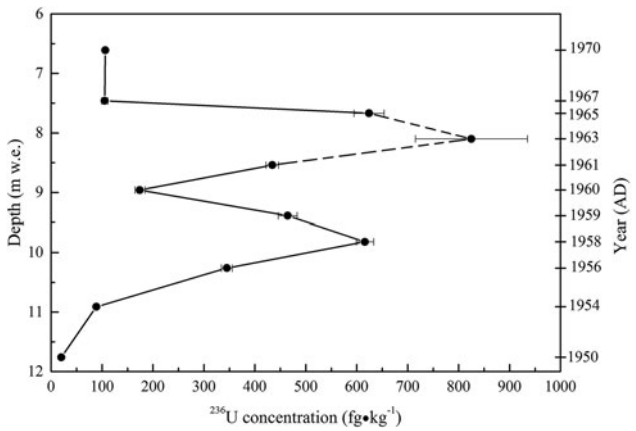

Fig. 3. Concentrations of ^{236}U in the Miaoergou ice core. The axes are identical to those in Figure 2. Error bars refer to 1 σ.

Figure 3 depicts the deposition rates of ^{236}U. Due to technique problems, one sample was lost during handling. Unfortunately, it turned out to be the sample with the presumed highest mass (or activity). We decided to extrapolate the missing value assuming the shape of the peak being identical to the shape of the ^{239}Pu peak. The reason is the same nuclear process that forms both radionuclides in an explosive scenario (neutron caption with uranium isotopes). Therefore, the ^{239}Pu/^{236}U ratios from the two neighbouring samples were used to estimate the missing ^{236}U value. We indicate the uncertainty in the described procedure using dashed lines in Figure 3. On the basis of this assumption, a total fallout of ^{236}U from NTW can be estimated to be 3.5×10^8 atoms·cm^{-2}. This value agrees rather well with 1.63×10^8 atoms·cm^{-2} (Wendel and others, 2013) from the Arctic site Svalbard 79.83°N based on the expected trend of deposition rate with latitude. However, as explained above for ^{239}Pu, also for ^{236}U the deposition rates are expected to vary largely from site to site.

Table 3 lists the ^{240}Pu/^{239}Pu atomic ratios in both the plutonium and uranium samples, as well as the ^{236}U/^{239}Pu atomic number ratios in the uranium samples. The values for ^{239}Pu/^{242}Pu atomic ratios are also listed, which were measured in the plutonium and uranium fractions to underlie the large variability. Within uncertainties, in all except one (sample 10), the ^{240}Pu/^{239}Pu ratios average ~0.18 ± 0.02. This value is well known to represent average fallout from the NWT where bomb debris from US and USSR tests were injected into the stratosphere, mixed due to the long residence time of ~2 years prior to re-entering the troposphere again and deposition on the Earth surface mostly by wet precipitation. Hence, no indication is found for debris from the nearby Lop Nor Chinese test site. Soil measurements in the vicinity of Lop Nor yielded average values of 0.158 (Bu and others, 2015).

Sample 10 indicated the deposition ~1953 ± 1 according to the cross-check result of multiple dating methods in the ice core. The first high-yield nuclear device (Ivy Mike. 5.7 Mt fission) was detonated in November 1952 at Enewetak Atoll in the Marshall Islands with an estimated locally deposited fission energy of 2.9 Mt (Lindahl and others, 2011). The mushroom cloud created by the explosion rose to an altitude of 37 km reaching the stratosphere (Machta and others, 1956). After the rapid transmission in the stratosphere and stratosphere–troposphere exchange, the fallout deposited globally. A higher ^{240}Pu/^{239}Pu ratio of 0.46 was observed for the Ivy test (Lindahl and others, 2011). A more recent study of nuclear weapons produced ^{236}U, ^{239}Pu and ^{240}Pu archived in a Porites Lutea coral from Enewetak Atoll (Froehlich and others, 2017) showed that in this archive the measured ^{240}Pu/^{239}Pu ratio was between 0.6 (1952) and 0.2 (1954) (i.e. significantly higher compared with younger samples) and the ^{236}U/^{239}Pu ratio varied for the same time period between 0.04 and 0.1 (i.e. lower than for younger samples). Both observations are in line with our data for sample 10 with the ratios for ^{240}Pu/^{239}Pu of 0.27 and for ^{236}U/^{239}Pu of 0.12, respectively.

The scatter of the ^{236}U/^{239}Pu ratios is larger than for the ^{240}Pu/^{239}Pu ratios. The average ^{236}U/^{239}Pu ratio of 0.27 ±

0.09, however, is in good agreement with information from the literature, e.g. 0.18–0.33 for an Arctic ice core (Wendel and others, 2013), 0.235 ± 0.014 from global fallout (Sakaguchi and others, 2009) or 0.05–0.50 for Stratospheric fallout (Ketterer and others, 2007). It is interesting to note that this ratio is significantly higher in aquatic systems, e.g. 1–12 in river water samples (Eigl and others, 2013) or ~0.7 in the deep Arctic Ocean [^{236}U data in Casacuberta and others (2016), Pu data unpublished]. This nicely reflects the fact that ^{236}U is extremely conservative in water, while Pu is not. Pu strongly adsorbs to surfaces, hence is depleted in water flows. This leads to higher values of the ^{236}U/^{239}Pu ratio.

4. CONCLUSIONS

Concentrations, atom ratios and the total deposition flux during NWT of ^{239}Pu, ^{240}Pu and ^{236}U were obtained for an ice core from eastern Tien Shan, Central Asia. The observed ^{240}Pu/^{239}Pu atom ratios were 0.18 ± 0.02, except for one sample, which represents the global fallout ratio of 0.18. No indication for emission from local sources (Lop Nor) was found. The ^{236}U/^{239}Pu ratios were between 0.12 and 0.43 (average 0.27), in good agreement with values from the literature. Our measured deposition rate for ^{239}Pu of 1.55×10^9 atoms·cm^{-2} during the NWT period lies within measured values for other sites in the NH though the scatter of reported values is quite large (factor of seven). The higher fallout of ^{239}Pu in eastern Tien Shan glacier may be ideal for defining the Anthropocene. The expected trend of deposition rates with latitude was not observed (lower values at higher latitudes), obviously due to local meteorological conditions that influence deposition rates. The measured ^{236}U deposition rate of 3.5×10^8 atoms·cm^{-2} agrees within the variability of such measurements with another measurement at an Arctic site (Svalbard, 79.83°N; 24.02°E; 750 m a.s.l.) of 1.6×10^8 atoms·cm^{-2} (Wendel and others, 2013).

ACKNOWLEDGEMENTS

The effort of the field personnel on the scientific expedition to the Miaoergou glacier in 2005 is highly appreciated. We thank for the support from E. Vogel and S. Szidat during a chemical procedure at the Bern University. The excellent performance of the AMS beam facility at ETH Zürich is highly appreciated. This work was supported by the Natural Science Foundation of China (grant numbers 41330526 and 41711530148), Chinese Academy of Sciences (grant number XDB03030101-4).

REFERENCES

Arienzo M and 11 others (2016) A method for continuous ^{239}Pu determination in Arctic and Antarctic Ice cores. *Environ. Sci. Technol.*, **50**(13), 7066–7073 (doi: 10.1021/acs.est6b01108)

Bloch S (1980) Some factors controlling the concentration of uranium in the world ocean. *Geochim. Cosmochim. Acta*, **44**, 373–377 (doi: 10.1016/0016-7037(80)90145-3)

Bu W, Ni Y, Guo Q, Zheng J and Uchida S (2015) Pu isotopes in soils collected downwind from Lop Nor: regional fallout vs. Global fallout. *Sci. Rep.*, **5**, 12261 (doi: 10.1038/srep12262)

Canfield D, Glazer A and Falkowski P (2010) The evolution and future of Earth's nitrogen cycle. *Science*, **330**(6001), 192–196 (doi: 10.1126/science.1186120)

Casacuberta N and 5 others (2014) A first transect of ^{236}U in the North Atlantic Ocean. *Geochim. Cosmochim. Acta*, **133**, 34–46 (doi: 10.1016/j.gca.2014.02.012)

Casacuberta N and 8 others (2016) First ^{236}U data from the Arctic Ocean and use of ^{236}U/^{238}U and ^{129}I/^{236}U as a new dual tracer. *Earth Planet Sci. Lett.*, **440**, 127–134

Chamizo E, Enamorado S, Garcia-Leon M, Suter M and Wacker L (2008) Plutonium measurements on the 1 MV AMS system at the Centro Nacional de Aceleradores (CNA). *Nucl. Instrum. Methods Phys. Res. B*, **266**, 4948–4954 (doi: 10.1016/j.nimb.2008.08.001)

Choppin G and Morgenstern A (2001) Distribution and movement of environmental plutonium. *Radioact. Environ.*, **1**, 91–105 (doi: 10.1016/S1569-4860(01)80009-7)

Christl M and 6 others (2012) A depth profile of uranium-236 in the Atlantic Ocean. *Geochim. Cosmochim. Acta*, **77**, 98–107 (doi: 10.1016/j.gca.2011.11.009)

Christl M and 6 others (2013) The ETH Zurich AMS facilities: performance parameters and reference materials. *Nucl. Instrum. Method B*, **294**, 29–38 (doi: 10.1016/j.nimb.2012.03.004)

Christl M and 6 others (2015a) Reconstruction of the ^{236}U input function for the Northeast Atlantic Ocean: implications for ^{129}I/^{236}U and ^{236}U/^{238}U-based tracer ages. *J. Geophys. Res. Oceans*, **120**, 7282–7299 (doi: 10.1002/2015JC011116)

Christl M and 10 others (2015b) Status of ^{236}U analyses at ETH Zurich and the distribution of ^{236}U and ^{129}I in the North Sea in 2009. *Nucl. Instrum. Method B*, **361**, 510–516 (doi: 10.1016/j.nimb.2015.01.005)

Crutzen P (2002) Geology of mankind. *Nature*, **415**, 23 (doi: 10.1038/415023a)

Crutzen P and Stoermer E (2000) The 'Anthropocene'. *Glob. Change Newsl.*, **41**, 17–18

Dai X, Christl M, Kramer-Tremblay S and Synal H-A (2011) Ultra-trace determination of plutonium in urine samples using a compact accelerator mass spectrometry system operating at 300 Kv. *J. Anal. At. Spectrom.*, **27**, 126–130 (doi: 10.1039/C1JA10264H)

Dunk R, Mills R and Jenkins W (2002) A reevaluation of the oceanic uranium budget for the Holocene. *Chem. Geol.*, **190**(1–4), 45–67 (doi: 10.1016/S0009-2541(02)00110-9)

Eigl R, Srncik M, Steier P and Wallner G (2013) ^{236}U/^{238}U and ^{240}Pu/^{239}Pu isotopic ratios in small (2 L) sea and river water samples. *J. Environ. Radioact.*, **116**, 54–58 (doi: 10.1016/j.jenvrad.2012.09.013)

Ford J, Price S, Cooper A and Waters C (2014) An assessment of lithostratigraphy for anthropogenic deposits. In Waters C, Zalasiewicz J, Williams M, Ellis M, Snelling A, eds. *A stratigraphical basis for the Anthropocene, geological society*, Special Publications, London, Vol. **395**, 55–89 (doi: 10.1144/SP395.12)

Froehlich M, Tims S, Fallon S, Wallner A and Fifield L (2017) Nuclear weapons produced ^{236}U, ^{239}Pu and ^{240}Pu archived in a Porites Lutea coral from Enewetak Atoll. *J. Environ. Radioact., in press* (doi: 10.1016/j.jenvrad.2017.05.009)

Gabrieli J and 8 others (2011) Contamination of Alpine snow and ice at Colle Gnifetti, Swiss/Italian Alps from nuclear weapons tests. *Atmos. Environ.*, **45**, 587–593 (doi: *10.1016/j.atmosenv.2010.10.039*)

Ketterer M, Hafer K, Jones V and Appleby P (2004) Rapid dating of recent sediments in Loch Ness: inductively coupled plasma mass spectrometric measurements of global fallout plutonium. *Sci. Total Environ.*, **322**(1–3), 221–229 (doi: 10.1016/j.scitotenv.2003.09.016)

Ketterer M, Groves A and Strick B (2007) ^{236}U inventories, ^{236}U/^{238}U, and ^{236}U/^{239}Pu: the stratospheric fallout signature, Goldschmidt Conference abstracts. *Geochim. Cosmochim. Acta*, **71**, A480

Koide M, Michel R, Goldberg E, Herron M and Langway C, Jr (1982) Characterization of radioactive fallout from pre- and post-moratorium tests to polar ice caps. *Nature*, **296**, 544–547 (doi: 10.1038/296544a0)

Koide M, Bertine K, Chow T and Goldberg F (1985) The ^{240}Pu/^{239}Pu ratio, a potential geochronometer. *Earth Planet. Sci. Lett.*, **72**, 1–8 (doi: 10.1016/0012-821X(85)90112-8)

Krey P and 5 others (1976) Mass isotopic composition of global fall-out pollution in soil. In *Transuranium nuclides in the environment*, ed. Horn W. IAEA-SM-199/39. IAEA, Vienna, 671–678.

Kudo A and 5 others (2000) Global transport rates and future prediction of hazardous materials: Pu and Cs – from Nagasaki to Canadian Arctic. *Water Sci. Technol.*, **42**, 163–169

Lewis S and Maslin M (2015) Defining the Anthropocene. *Nature*, **519**, 171–180 (doi: 10.1038/nature14258

Lindahl P and 5 others (2011) Sources of plutonium to the tropical Northwest Pacific Ocean (1943–1999) identified using a natural coral archive. *Geochim. Cosmochim. Acta*, **75**, 1346–1356 (doi: 10.1016/j.gca.2010.12.012)

Liu Y and 5 others (2011) High-resolution trace element records of an ice core from the eastern Tien Shan, Central Asia, since 1953 AD. *J. Geophys. Res.*, **116**, D12307 (doi: 10.1029/2010JD015191)

Machta L, List R and Hubert L (1956) World-wide travel of atomic debris. *Science*, **124**, 474–477

Micholas N, Coop K and Estep R (1992) *Capability and limitation study of DDT passive-active neutron waste assay instrument*. Los Alamos National Laboratory, Los Alamos, LA-12237-MS

Monastersky R (2015) The human age. *Nature*, **519**, 144–147 (doi: 10.1038/519144a)

Olivier S (2004) *Atmospheric and climate history of the past two centuries from Belukha ice core, Siberian Altai*. Ph.D. thesis, University of Bern. (And personal communication from S Olivier, 2013)

Olivier S and 8 others (2004) Plutonium from global fallout recorded in an ice from the Belukha glacier, Siberian Altai. *Environ. Sci. Technol.*, **38**(24), 6507–6512 (doi: 10.1021/es0492900)

Perkins R and Thomas C (1980) Worldwide fallout. US DOE/TIC-22800. In Hanson W. C. ed. *Transuranic elements in the environment*. Office of Health and Environmental Research, Washington DC, 53–82.

Ruddiman W, Ellis E, Kaplan J and Fuller D (2015) Defining the epoch we live in. *Science*, **348**, 38–39 (doi: 10.1126/science.aaa7297)

Sakaguchi A and 8 others (2009) First results on ^{236}U levels in global fallout. *Sci. Total Environ.*, **407**, 4238–4242 (doi: 10.1016/j.scitotenv.2009.01.058)

Sakaguchi A and 7 others (2012) Uranium-236 as a new oceanic tracer: a first depth profile in the Japan Sea and comparison with caesium-137. *Earth Planet. Sci. Lett.*, **333–334**, 165–170 (doi: 10.1016/j.epsl.2012.04.004)

Steier P and 14 others (2008) Natural and anthropogenic ^{236}U in environmental samples. *Nucl. Instrum. Methods Phys. Res. B*, **266**, 2246–2250 (doi: 10.1016/j.nimb.2008.03.002)

Steffen W, Crutzen J and McNeill J (2007) The Anthropocene: are humans overwhelming the great forces of nature? *Ambio*, **36**, 614–621

Vockenhuber C and 6 others (2011) The potential of He stripping in heavy ion AMS. *Nucl. Instrum. Method B*, **294**, 382–386 (doi: 10.1016/j.nimb.2012.01.014)

Wang C and 7 others (2014) ^{210}Pb dating of the Miaoergou ice core from the eastern Tien Shan Mountains, China. *Ann. Glaciol.*, **55** (66), 105–110 (doi: 10.3189/2014AoG66A151)

Waters C and 5 others (2014) *A stratigraphical basis for the Anthropocene*. Special Publications, Vol. **395**. London, Geological Society. Available at: http://sp.lyellcollection.org/content/395/1

Waters C and 10 others (2015) Can nuclear weapons fallout mark the beginning of the Anhropoene Epoch? *Bull. At. Sci.*, **71**(3), 46–57 (doi: 10.1177/0096340215581357)

Waters C and 23 others (2016) The Anthropocene is functionally and stratigraphically distinct from the Holocene. *Science*, **351**(6269), 137 (doi: 10.1126/science.aad2622)

Wendel C and 7 others (2013) Chronology of Pu isotopes and ^{236}U in an Arctic ice core. *Sci. Total Environ.*, **461–462**, 734–741 (doi: 10.1016/j.scitotenv.2013.05.054)

Winkler S, Steier P and Carilli J (2012) Bomb fall-out ^{236}U as a global oceanic tracer using an annually resolved coral core. *Earth Planet Sci. Lett.*, **359–360**, 124–130 (doi: 10.1016/ j.epsl.2012.10.004)

Wolfe A and 10 others (2013) Stratigraphic expressions of the Holocene-Anthropocene transition revealed in sediments from remote lakes. *Earth Sci. Rev.*, **116**, 17–34 (doi: 10.1016/j.earscirev.2012.11.001)

Yang X, North R and Romney C (2000) CMR Nuclear Explosion Database (Revision 3), CMR Technical Report CMR-00/16; Center for Monitoring Research, Arlington, VA

Zalasiewicz J, Kryza R and Williams M (2014) The mineral signature of the Anthropocene. In Waters C, Zalasiewicz J, Williams M, Ellis M, Snelling A eds. *A stratigraphical basis for the Anthropocene, geological society*. Special Publications, London, **395**, 109–117 (doi: 10.1144/SP395.2)

Zalasiewicz J and 25 others (2015) When did the Anthropocene begin? A mid-twentieth century boundary level is stratigrapgically optimal. *Q. Inter.*, **383**, 196–203 (doi: 10.1016/j.quaint.2014.11.045)

MS received 17 January 2017 and accepted in revised form 29 August 2017